Ocular phenotype analysis of a family with biallelic mutations in the BEST1 gene.

Sharon, Dror; Al-Hamdani, Sermed; Engelsberg, Karl; Mizrahi-Meissonnier, Liliana; Obolensky, Alexey; Banin, Eyal; Sander, Birgit; Jensen, Hanne; Larsen, Michael; Schatz, Patrik

Published in:
American Journal of Ophthalmology

DOI:
10.1016/j.ajo.2013.12.010

2014

ABSTRACT

Purpose: To investigate the genetic cause and perform a comprehensive clinical analysis of a Danish family with autosomal recessive bestrophinopathy. To investigate whether Bestrophin may be expressed in normal human retina.
Design: Retrospective clinical and molecular genetic analysis and immunohistochemical observational study.
Methods: Setting: National referral center. Participants: A family with five individuals and biallelic *BEST1* mutations, and enucleated eyes from two individuals with non-affected retinas. Observation procedures: Molecular genetic analysis included sequencing of *BEST1* and cosegregation analysis. Clinical investigations included electro-oculography, full-field electroretinography, multifocal electroretinography, spectral domain optical coherence tomography and fundus autofluorescence imaging. Immunohistochemical analysis was performed. Main Outcome Measures: *BEST1* mutations, imaging findings, electroretinography amplitudes and implicit times.
Results: The index case was compound heterozygous for p.A195V and a novel 15 base pair deletion leading to p.Q238L. The index case at age 10 demonstrated multifocal vitelliform changes that were hyperautofluorescent, cystoid macular edema in the inner nuclear layer, no light rise in the electro-oculography and a reduced central but preserved peripheral retinal function by multifocal electroretinography. Full-field electroretinography demonstrated a reduced rod response and inner retina dysfunction. Retinal structure was normal in all three family members who carried a sequence change in *BEST1*. Electro-oculography light peak was reduced in both the mother and sister (heterozygous for p.Q238L). Immunohistochemistry could not confirm the presence of Bestrophin in normal human retina.
Conclusions: Because of a relatively well-preserved retinal function, autosomal recessive bestrophinopathy may be a suitable first candidate, among the *BEST1*-related ocular conditions, for gene replacement therapy.

Ocular phenotype analysis of a family with biallelic mutations in the *BEST1* gene

Dror Sharon[1], Sermed Al-Hamdani[2,3], Karl Engelsberg[4], Liliana Mizrahi-Meissonnier[1], Alexey Obolensky[1], Eyal Banin[1], Birgit Sander[2], Hanne Jensen[3], Michael Larsen[2,3,5], Patrik Schatz[2,3,4]

[1] Department of Ophthalmology, Hadassah-Hebrew University Medical Center, Jerusalem, Israel.

[2] Department of Ophthalmology, Glostrup Hospital, Glostrup, Denmark.

[3] National Eye Clinic, Kennedy Center, Glostrup, Denmark.

[4] Department of Ophthalmology, Clinical Sciences, Scane County University Hospital, University of Lund, Sweden.

[5] Faculty of Health and Medical Sciences, University of Copenhagen, Copenhagen, Denmark.

Statement: Each of the coauthors has seen and agrees with each of the changes made to this manuscript in the revision and to the way his or her name is listed.

Short title: Phenotype in family with biallelic mutations in *BEST1*

Correspondence to:

Patrik Schatz, Department of Ophthalmology, Clinical Sciences, Scane County University Hospital, 22185 Lund, Sweden. Telephone number: +46 46 171000.

E mail: patrik.schatz@med.lu.se

Supplemental Material available at AJO.com

INTRODUCTION

Different mutations in the *BEST1* gene can cause a variety of ocular phenotypes ranging from isolated vitelliform macular degeneration (due to disturbed function of the retinal pigment epithelium) which manifests as a reduced light peak in the electro-oculogram as in Best disease, to widespread retinal degeneration as in autosomal recessive bestrophinopathy and further to widespread ocular manifestations as in autosomal dominant vitreoretinochoroidopathy.[1-5] The phenotypes described as autosomal dominant and autosomal recessive retinitis pigmentosa resemble those of autosomal dominant vitreoretinochoroidopathy and autosomal recessive bestrophinopathy, respectively.[6] Although a large number of patients with *BEST1* mutations have been recently reported with different phenotypes, no clear genotype-phenotype correlation can be obtained for *BEST1*-associated ocular diseases. This can be partially explained by the considerable variability in disease expressivity among patients who carry the same *BEST1* disease-causing mutation.

Autosomal recessive bestrophinopathy seems to be intermediate in severity among the bestrophinopathies and is characterized by biallelic mutations in *BEST1*, the absence of a light rise in the electro-oculography, reduced full-field electroretinogram, pigment irregularities and vitelliform changes in the posterior pole of the fundus and may include cystoid macular edema and angle-closure glaucoma.[4] However, other biallelic mutations may manifest as classical Best disease with no signs of generalized involvement of the retina except for a reduced electro-oculography light rise.[3] Furthermore, angle-closure glaucoma was also recently described in classical Best disease.[7]

The electro-oculogram measures the resting potential across the retinal pigment epithelium. The clinical hallmark of Best disease and other *BEST1*-associated retinopathies is a reduction of the electro-oculography light rise, which indicates a disturbed function of the retinal pigment epithelium. This reduction is consistently pronounced in autosomal recessive bestrophinopathy, where the light rise in the electro-oculogram may be absent or nearly absent.[4] The gene product of *BEST1* was previously postulated to act as an calcium-sensitive chloride channel in the basolateral retinal pigment epithelium however a recent study showed that bestrophin is localised in the endoplasmic reticulum membrane, close to the cell membrane.[8] In vitro studies, in which cells were transfected with mutant and wild type bestrophin and chloride currents were measured, have shown that certain recessive mutations associated with autosomal recessive bestrophinopathy (mutations p.R141H and p.P152A) resulted in diminished chloride currents compared to wild type.[4] Subsequent cotransfection with wild type bestrophin resulted in currents that were not different from cells transfected with wild type protein alone, consistent with a recessive nature of disease.[4] By contrast, cotransfection with wild type protein did not restore chloride currents in cells that were previously transfected with mutated bestrophin due to dominant mutations (p.W93C and p.R218C). Thus, lack of channel conductance may underlie or contribute to the reduction or absence of a light rise in the electro-oculogram and may be a pathogenic mechanism of particular relevance in autosomal recessive bestrophinopathy.

In this study we present a detailed clinical and genetic investigation of a family with biallelic mutations in *BEST1*, in an attempt to gain additional information on the mechanism by which different *BEST1* mutations cause a variety of ocular phenotypes. The biallelic form of *BEST1*-associated retinopathy is of particular interest, because an animal model exists, namely canine multifocal retinopathy for which gene therapy has shown

sustained therapeutic effect (Guziewicz K, et al. IOVS 2013;54:ARVO E-Abstract 5965).[9] Although the autosomal recessive bestrophinopathy phenotype has been presented in many papers since its original description by Burgess et al. in 2008,[4] we herein present and evaluate several novel molecular genetic and clinical aspects in members of a family with biallelic mutations in *BEST1*. These new findings and investigations include: (1) The presence of three sequence alterations in *BEST1*, one of which is a novel deletion of 15 nucleotides, (2) Data on choroidal thickness and anterior chamber angle and (3) Evaluation of the luminance-response series in the full-field electroretinogram. Finally, as structural and functional data indicated involvement of the inner retina in autosomal recessive bestrophinopathy, we performed immunohistochemistry to investigate whether Bestrophin may be expressed in the normal human retina.

PATIENTS AND METHODS

This retrospective study included a 10 year-old index case with vitelliform maculopathy and five first-degree relatives (Fig. 1). In addition, for immunohistochemical studies we used two adult human eyes, which had been enucleated because of a malignant tumor and ocular trauma. Prior to donation of a blood sample for DNA analysis, informed consent was obtained from all patients and family members who participated in this study. Ethical permission for DNA analysis and clinical investigation in patients with hereditary retinal degeneration was obtained from the central ethical review board at Lund University, Sweden. Institutional review board approval is not granted for retrospective studies in Denmark. In Denmark, institutional review boards to not provide waivers. This was not a systematic evaluation of a treatment or a device. The tenets of the Declaration of Helsinki were followed and all federal or state laws in the countries (Israel, Denmark, Sweden) involved in the study.

Molecular genetic methods

Genomic DNA was extracted from peripheral blood of all family members using standard procedures. Molecular genetic analysis included Sanger sequencing of the *BEST1* coding region and intron-exon junctions and a cosegregation analysis in the studied family. Primers for exons 1-3 and 5-11 of *BEST1* were previously reported.[10] Primers for exon 4 were: forward 5'-AGAAAGCTGGAGGAGCCGA-3' and reverse 5'-TCCACCCATCTTCCATTCCTGC-3'. The predicted effect of a sequence change on splicing was evaluated using the splice-site prediction by neural network platform (http://www.fruitfly.org/seq_tools/splice.html; accessed: September 3, 2013). The possible pathogenicity of missense changes was evaluated using PolyPhen-2 (http://genetics.bwh.harvard.edu/pph2/; accessed: September 3, 2013), MutationTaster (http://www.mutationtaster.org; accessed: September 3, 2013), and SIFT (http://sift.jcvi.org; accessed: September 3, 2013).

Clinical investigations

Investigations included standard clinical examination, multifocal electroretinography, fundus autofluorescence imaging, and spectral domain optical coherence tomography, full-field electroretinography and electro-oculography as described previously,[11-13] with some modification as follows.

Electrophysiological examinations were conducted at Kennedy Centre, Denmark according to the standards given by International Society of Clinical Electrophysiology in

Vision,[14-16] with one exception: Dawson-Trick-Litzkow[17] electrodes were used instead of Burian-Allen contact lens electrodes because of contact lens intolerance in the index case and the choice of using the same method in all family members. For both electro-oculography and full-field electroretinography, we used a Viking 5.0 Ganzfeld dome (Nicolet Biomedical Instruments, Madison, Wisconsin), with a light-emitting diode for light stimulation. The Ganzfeld dome was equipped with an infrared camera to monitor the position of the eye during the examination.

In addition, the dark-adapted full-field electroretinography was extended to include an intensity response series outside the standard given by the International Society of Clinical Electrophysiology in Vision, with seven stimuli intensities between -1.5 and +1.5 log units with a 0.5 log unit interval, where the standard flash luminance of 3.0 candela-seconds per square meter corresponds to 1.0 log units. Each response represented an average of at least two measurements of comparable size and shape, if possible.

In both full-field electroretinography and multifocal electroretinography, the reference electrode was positioned inferior to the lateral canthus and the ground electrode on the earlobe. The examined eye was locally anesthetized with oxybuprocaine 0.4% prior to positioning the Dawson-Trick-Litzkow electrode.

Multifocal electroretinography was performed using VERIS 4.0 (Electro-Diagnostic Imaging, San Diego, California, USA) with charge-coupled device camera. The stimulus pattern of multifocal electroretinography consisted of 103 hexagons. The multifocal electroretinography examination was subdivided into 16 segments of 30 seconds. A short break of 2-5 seconds was given after each segment. We used 17 percent averaging from neighbouring hexagons and two iterations of artifact removal when calculating multifocal electroretinography ring averages and presenting trace plots.

Anterior segment optical coherence tomography (Visante OCT, Carl Zeiss Meditec, Jena, Germany) and/or Scheimpflug Pentacam (Oculus Optikgeräte GmbH, Wetzlar, Germany) was performed to visualize and measure the anterior chamber angle and the subfoveal choroidal thickness was examined using spectral domain optical coherence tomography and enhanced depth imaging and measured as described previously.[18]

Immunohistochemistry

Eyes from two unrelated individuals with no known *BEST1*-related disease were enucleated due to a malignant choroidal melanoma or ocular trauma. The malignant tumor was located well away from the sampled tissue. Samples were fixed in 4% paraformaldehyde, embedded on paraplast and cut. After deparaffinization and rehydration, sections were incubated in a decloacking chamber (Biocare Medical, USA) with 10mM citrate buffer (pH 6.0) at 125°C for 10min. Hereafter they were rinsed several times with phosphate buffered saline, blocked with phosphate buffered saline containing 1% bovine serum albumin, 0.1% triton-X100 and 10% of normal donkey serum, and subsequently incubated overnight at 4°C with anti-Bestrophin 1 primary antibody (mouse monoclonal, 1:50; Novus Biologicals, Littleton, Colorado). After washing in phosphate buffered saline, the secondary antibody was applied for 1 hour (DyLightTM 549 AffiniPure Donkey Anti-Mouse IgG, 1:250; Jackson ImmunoResearch Laboratories, Inc., West Grove, Pennsylvania). Nuclei were counterstained with 4,6-diamidino-2-phenylindole–containing mounting medium (Vector Laboratories, Burlingame, California). To determine the specificity of the antigen–antibody reaction, corresponding negative controls with the secondary antibody alone were performed. Observation and photography were performed

using a fluorescent microscope (Olympus BX41, Japan) equipped with a DP70 digital camera.

RESULTS

Mutation analysis

Sequencing analysis of *BEST1* in the index case (a 10 year-old boy, II:3, Fig. 1) revealed three heterozygous sequence changes (Supplementary Table 1). Two sequence changes are missense (e.g. affect only one amino-acid) and were previously reported by others: the p.A195V change (Alanine at position 195 is replaced by Valine) was described previously in Best disease, in autosomal recessive bestrophinopathy, and in multifocal Best disease and the p.A357V change (Alanine at position 357 is replaced by Valine) was reported in patients with Best disease.[19-23] In addition, we identified a novel deletion of 15 nucleotides (termed c.713del15; the deletion includes the last two nucleotides of exon 6 and the first 13 nucleotides of intron 6; Fig. 1). Although deletions that involve the exon-intron junction are likely to affect mRNA splicing, the deletion we identified is unique due to sequence similarities between the mutated and wild-type sequence and is thus not predicted to affect the normal splicing of exon 6 (as predicted by splicing prediction tools), but instead results in a novel missense change (p.Q238L). Based on the reported allele frequency and the pathogenicity prediction for each sequence changes (Supplementary Table 1), we predict that p.A195V and p.Q238L are disease-causing mutations, while p.A357V is a rare nonpathogenic variant. We examined *BEST1* alleles in all five family members and were able to determine the segregating alleles in the family (Fig. 1). The index case is compound heterozygous for p.A195V (which was inherited from the father) and p.Q238L (in cis with p.A357V, inherited from the mother). None of the two siblings inherited this combination of alleles, the sister inherited the p.Q238L-p.A357V allele and the brother inherited two normal copies of the *BEST1* gene (Fig. 1).

Clinical findings

The index case at the age of 10 years had widespread vitelliform changes in the posterior pole (Fig. 2- upper panel) that were hyperautofluorescent (Fig. 2- middle panel), indicating the presence and accumulation of retinoid derivatives such as lipofuscin. Photoreceptor outer segments were elongated in a precipitate-like manner and focal mounds were present on Bruch´s membrane, these structures being separated by subretinal fluid. Cystoid macular edema localized in the inner nuclear layer (Fig. 2- lower panel; arrows indicate the limits of the inner nuclear layer). Multifocal electroretinography demonstrated a reduced central but preserved paracentral retinal function in the right eye, as demonstrated by the analysis of ring ratios given as the ratio of the responses from the center (rings 1-2) versus those from the periphery (rings 3-6) (Table 1 and Fig. 3). Analysis of absolute amplitudes in these rings demonstrated a more pronounced amplitude reduction throughout the field in the left eye, as compared to the right eye. There was no consistent light rise in the electro-oculography (Table 1 and Fig. 4).

Full-field electroretinography indicated reduced rod driven response in the index case compared to other family members while the cone driven responses were better preserved, except for a delay in 30 Hz flicker implicit time (Fig. 5 and Table 2). A further

evaluation of retinal function with an intensity response series in the dark adapted full-field electroretinography demonstrated lower amplitude in the index case only at the dimmest stimulus luminance, corresponding to the rod dominated response, however with increasing stimulus luminance, and thus increasing contribution from cones, the response was comparable to that of other family members (right eye of index case) or even exceeded that other family members (left eye of index case) (Table 2, Figs. 6,7).

There were no signs of angle closure glaucoma except for a narrow chamber angle and shallow anterior chamber in the mother (Table 1). Intraocular pressure was not elevated. Subfoveal choroidal thickness was increased in the mother but normal in the other individuals (Table 1). Retinal structure was normal in all three family members who carried a sequence change in *BEST1*, however the mother and sister demonstrated slightly reduced cone driven central responses by multifocal electroretinography (Fig. 3). Electro-oculography light rise was present however the light peak was reduced in the mother and sister (both heterozygous for p.Q238L), while the father (heterozygous for the p.A195V mutation) demonstrated a normal electro-oculography light peak (Fig. 4).

Immunohistochemistry

Our clinical analysis displayed a clear inner retinal pathology that might be caused directly by abnormal expression of Bestrophin in the inner retina or by a secondary effect due to morphological change in the junction between retinal pigment epithelium and photoreceptors and accumulation of fluid due to the abnormal function of Bestrophin in the retinal pigment epithelium. The presence of bestrophin in the retinal pigment epithelium is well-established in different organisms, however no information is available to determine if Bestrophin is expressed, even at low levels, in the human inner retina. We therefore performed immunohistochemistry on two human retinas, in both cases with 4,6-diamidino-2-phenylindole displayed the nuclear layers with their normal morphology. Bestrophin immunohistochemistry displayed a unique and intense labeling of the retinal pigment epithelium layer with no traces of expression in other retinal cells (Fig. 8).

DISCUSSION

The distinction between *BEST1* mutations that result in dominant or recessive inheritance is not well established, and expression and penetrance of specific mutations may be affected by other unknown environmental or genetic factors. The p.A195V mutation was previously reported heterozygously in patients with Best disease,[19, 21] multifocal vitelliform dystrophy,[20] autosomal recessive bestrophinopathy,[22] and in an unaffected individual.[20] In the family studied here, p.A195V does not seem to cause any manifestations of Best disease (including a normal electro-oculography light rise and light peak) in a heterozygous analyzed family member (father), and thus acts as a recessive mutation or a nonpenetrant dominant mutation. On the other hand, the novel deletion resulting in p.Q238L heterozygously leads to a reduced electro-oculography light peak but does not seem to be penetrant for other manifestations of Best disease (mother and one sibling). Interestingly, the compound heterozygous/biallelic state with both mutations leads to autosomal recessive bestrophinopathy including no light rise in the electro-oculography, reduced rod driven response in the full-field electroretinography and cystoid macular edema in the inner nuclear layer (index case). Thus the classic distinction between autosomal recessive and autosomal dominant models of inheritance may not be easily

applied to bestrophinopathies, where dosage effects of available Bestrophin protein may be more important in determining the eventual disease in a patient.

Cystoid macular edema was also described in an autosomal recessive bestrophinopathy case,[24] and extensively analyzed, including the effect of treatment of macular edema with carbonic anhydrase inhibitors, by Boon et al in a cohort of patients with autosomal recessive bestrophinopathy.[25] Carbonic -inhibitor acetazolamide reduces cystoid macular edema in autosomal recessive bestrophinopathy through an interaction with membrane-bound carbonic anhydrase in the retinal pigment epithelium and/or Müller's cells, and/or intracellular carbonic anhydrase in the retina. An inhibition of intracellular carbonic anhydrase leads to intracellular acidification, which activates a transepithelial, apical-to-basolateral chloride transport in the retinal pigment epithelium, with water following passively. It was suggested that the effect of carbonic anhydrase inhibitors such as acetazolamide on cystoid macular edema in autosomal recessive bestrophinopathy is probably indirect, through an inhibition of retinal carbonic anhydrase activity, and not through direct targeting of Bestrophin.

Photoreceptor outer segment layer thickening may be an unspecific consequence of serous neurosensory retinal detachment, as described in central serous chorioretinopathy, and recently in Best disease by us.[26, 27] However, cystoid macular edema is not a feature of classical Best disease and thus seems to distinguish autosomal recessive bestrophinopathy from Best disease. The predilection of edema for the inner nuclear layer may reflect a spill over from subretinal fluid, which in turn probably results from a deficient pumping mechanism of the retinal pigment epithelium. However, the inner nuclear layer is a locus for edema in conditions with different pathophysiology, such as vascular leakage and breakdown of the inner blood retina barrier as in diabetic macular edema and in multiple sclerosis.[28, 29] The plexiform layers surrounding the inner nuclear layer contain networks of microglia that seem to form a diffusion barrier. There may also be a primary involvement of Müller glia in the genesis of the inner nuclear layer edema in multiple sclerosis,[29] and by analogy it is tempting to speculate that Bestrophin may be expressed in the inner retina and that a failure of potassium and chloride transport across the cell membrane results in edema in this retinal layer in autosomal recessive bestrophinopathy. This could potentially explain the alterations in the full-field electroretinography in autosomal recessive bestrophinopathy, as the Muller cells alongside with bipolar cells are believed to act as the primary generators of the full-field electroretinography b wave. In fact, a recent study by Zhu et al in 2010 demonstrated *best1* promoter activity in progenitors of Muller cells in transgenic mice, indicating that this gene may be expressed in Muller cells at least during certain stages of retinal development.[30] Our immunohistochemistry analysis, however, did not demonstrate any Bestrophin labelling in the inner retina in samples from 2 humans.

The primary involvement of the retinal pigment epithelium in Best disease and autosomal recessive bestrophinopathy seems to lead to a secondary retinal macular degeneration which in Best disease progresses through various stages, where the initial stages may include edema and subretinal fluid and the final stages feature atrophy and retinal thinning. We investigated the hypothesis whether this primary affection of the retinal pigment epithelium would lead to a secondary choroidal degeneration, however measurement of subfoveal choroidal thickness with enhanced depth imaging did not reveal any thinning in the present study.

A further analysis of retinal function by full-field electroretinography, outside the standards given by the International Society of Clinical Electrophysiology in Vision, included a luminance-response series. Similar series have been investigated previously, for example by Rufiange et al. 2003, who performed a systematic analysis of several defined response parameters (albeit in the light adapted state as opposed to our series which was performed in the dark adapted state) in controls and in selected cases of retinal degeneration.[31] In general, for progressively brighter stimuli, there is a steady increase in the response until a plateau is reached, after which a further increase in stimulus luminance will cause a decrease in the response, a phenomenon known as the photopic hill. The slope of this hill probably results from complex mechanisms involved such as the interaction of ON and OFF-bipolar cell responses.

In the compound heterozygous index case, a reduced response was seen only for the dimmest stimulus luminance, however with increasing stimulus luminance, the response did not differ from that of other family members (right eye of index case) or exceeded that of other family members (left eye of index case) (Figs. 6,7). This may indicate a decrease in retinal sensitivity and reduced rod function in the index case. Furthermore, considering that the full-field electroretinography b wave is generated by bipolar cells and Muller cells, it may indicate a dysfunction in the inner retina. Thus electrophysiological findings are consistent with a secondary effect of the mutated bestrophin on the inner retina. This is also consistent with the structural findings based on optical coherence tomography in the index case presented here and in previous publications.[24, 25]

Limitations of the present study include small sample size and the use of Dawson-Trick-Litzkow electrode instead of a contact lens Burian Allen electrode for electrophysiology. The former may lead to less precise, more noisy recordings with blink artefacts and reduced amplitudes,[32] as compared to the Burian Allen contact lens electrode. Interocular asymmetry can also be caused by asymmetrically placed Dawson-Trick-Litzkow electrodes or periocular muscle or lid muscle activity. Furthermore, with the most recent Burian Allen contact lenses, an infrared camera is mounted on the contact lens, which enables fundus viewing during a multifocal electroretinography recording. This allows for control of fixation and the examiner can verify that all parts of the multifocal electroretinography hexagonal array are projected onto the correct parts of the fundus. Instead we monitored the pupil for fixation with infrared camera during both full-field electroretinography and multifocal electroretinography, thus the projection of the multifocal electroretinography hexagonal array could not be confirmed through direct visualization. We could assess indirect signs of proper alignment, such as preserved peripheral responses throughout the circumference in the right eye of the index case.

The methodological approach of the present study is an extensive clinical investigation of relevant parameters followed by inter-individual comparison within a family with well-defined genotypes keeping in mind that apparently normal family members should also be sufficiently examined to determine the type of inheritance and nature of disease. We suggest that this is a fruitful methodology in the study of genotype-phenotype associations in hereditary retinal disorders, and has been used previously by us and others, to find new disease entities among hereditary eye disorders.[3, 4, 33, 34]

To conclude, we present a comprehensive clinical and molecular genetic evaluation of a family with biallelic mutations in *BEST1*. The compound heterozygous index case at age 10 was found to have a surprisingly well-preserved cone function (by both full-field electroretinography and multifocal electroretinography) and, to some degree, rod function. This indicates that such patients may be suitable candidates for future gene replacement therapy until at least 10 years of age and perhaps further. Such cohorts of autosomal recessive bestrophinopathy patients were described recently.[25, 35] The suggestion can be made that this subpopulation of *BEST1*-associated ocular diseases, featuring biallelic mutations and recessive nature of disease, and having well-preserved retinal function by electrophysiology, should be first candidates for gene therapy in clinical trials on *BEST1*-associated diseases.

ACKNOWLEDGEMENTS

a. Funding/support: Grants from the Swedish Society of Medicine, Eye Foundation, Dag Lenard Foundation, Foundation for the visually impaired in the Skane County.
b. Financial disclosures: None of the authors have any financial disclosures.
c. Contributions to Authors:
Design of the study (DS, SAH, ML, PS,).
Conduct of the study (SAH, KE, LMM, AO, BS, HJ, ML, PS).
Collection, management, analysis, and interpretation of the data (DS, SAH, KE, LMM, EB, AO, BS, HJ, ML, PS).
Preparation, review and approval of the manuscript (DS, SAH, KE, LMM, EB, AO, BS, HJ, ML, PS).
d. Other acknowledgement: We appreciate the technical assistance with imaging modalities provided by Ms. Hajer Ahmad Al-Abaiji at the Department of Ophthalmology, Glostrup Hospital, Glostrup, Denmark and for the technical assistance regarding immunohistochemistry by Karin Arnér and for photographic assistance with the preparation of figures by Johnny Ring, both at the Department of Ophthalmology, Clinical Sciences, Scane County University Hospital, University of Lund, Sweden.

REFERENCES

1. MacDonald IM, Lee T. Best Vitelliform Macular Dystrophy. In: GeneReviews [Internet]. Available at: http://www.ncbi.nlm.nih.gov/books/NBK1167/. Accessed: December 4, 2013.
2. Yardley J, Leroy BP, Hart-Holden N, et al. Mutations of VMD2 splicing regulators cause nanophthalmos and autosomal dominant vitreoretinochoroidopathy (ADVIRC). *Invest Ophthalmol Vis Sci* 2004;45(10):3683-3689.
3. Bitner H, Mizrahi-Meissonnier L, Griefner G, Erdinest I, Sharon D, Banin E. A homozygous frameshift mutation in BEST1 causes the classical form of Best disease in an autosomal recessive mode. *Invest Ophthalmol Vis Sci* 2011;52(8):5332-5338.
4. Burgess R, Millar ID, Leroy BP, et al. Biallelic mutation of BEST1 causes a distinct retinopathy in humans. *Am J Hum Genet* 2008;82(1):19-31.
5. Burgess R, MacLaren RE, Davidson AE, et al. ADVIRC is caused by distinct mutations in BEST1 that alter pre-mRNA splicing. *J Med Genet* 2009;46(9):620-625.
6. Davidson AE, Millar ID, Urquhart JE, et al. Missense mutations in a retinal pigment epithelium protein, bestrophin-1, cause retinitis pigmentosa. *Am J Hum Genet* 2009;85(5):581-592.
7. Wittstrom E, Ponjavic V, Bondeson ML, Andreasson S. Anterior segment abnormalities and angle-closure glaucoma in a family with a mutation in the BEST1 gene and Best vitelliform macular dystrophy. *Ophthalmic Genet* 2011;32(4):217-227.
8. Gomez NM, Tamm ER, Straubeta O. Role of bestrophin-1 in store-operated calcium entry in retinal pigment epithelium. *Pflugers Arch* 2013;465(4):481-495.
9. Guziewicz KE, Slavik J, Lindauer SJ, Aguirre GD, Zangerl B. Molecular consequences of BEST1 gene mutations in canine multifocal retinopathy predict functional implications for human bestrophinopathies. *Invest Ophthalmol Vis Sci* 2011;52(7):4497-4505.
10. Petrukhin K, Koisti MJ, Bakall B, et al. Identification of the gene responsible for Best macular dystrophy. *Nat Genet* 1998;19(3):241-247.
11. Schatz P, Bitner H, Sander B, et al. Evaluation of macular structure and function by OCT and electrophysiology in patients with vitelliform macular dystrophy due to mutations in BEST1. *Invest Ophthalmol Vis Sci* 2010;51(9):4754-4765.
12. Andersen MK, Christoffersen NL, Sander B, et al. Oligocone trichromacy: clinical and molecular genetic investigations. *Invest Ophthalmol Vis Sci* 2010;51(1):89-95.
13. Wittstrom E, Ekvall S, Schatz P, Bondeson ML, Ponjavic V, Andreasson S. Morphological and functional changes in multifocal vitelliform retinopathy and biallelic mutations in BEST1. *Ophthalmic Genet* 2011;32(2):83-96.
14. Bach M, Hawlina M, Holder GE, et al. Standard for pattern electroretinography. International Society for Clinical Electrophysiology of Vision. *Doc Ophthalmol* 2000;101(1):11-18.
15. Marmor MF, Zrenner E. Standard for clinical electro-oculography. International Society for Clinical Electrophysiology of Vision. *Doc Ophthalmol* 1993;85(2):115-124.
16. Hood DC, Bach M, Brigell M, et al. ISCEV standard for clinical multifocal electroretinography (mfERG) (2011 edition). *Doc Ophthalmol* 2012;124(1):1-13.
17. Dawson WW, Trick GL, Litzkow CA. Improved electrode for electroretinography. *Invest Ophthalmol Vis Sci* 1979;18(9):988-991.

18. Li XQ, Larsen M, Munch IC. Subfoveal choroidal thickness in relation to sex and axial length in 93 Danish university students. *Invest Ophthalmol Vis Sci* 2011;52(11):8438-8441.
19. Lotery AJ, Munier FL, Fishman GA, et al. Allelic variation in the VMD2 gene in best disease and age-related macular degeneration. *Invest Ophthalmol Vis Sci* 2000;41(6):1291-1296.
20. Boon CJ, Klevering BJ, den Hollander AI, et al. Clinical and genetic heterogeneity in multifocal vitelliform dystrophy. *Arch Ophthalmol* 2007;125(8):1100-1106.
21. Kramer F, Mohr N, Kellner U, Rudolph G, Weber BH. Ten novel mutations in VMD2 associated with Best macular dystrophy (BMD). *Hum Mutat* 2003;22(5):418.
22. Gerth C, Zawadzki RJ, Werner JS, Heon E. Detailed analysis of retinal function and morphology in a patient with autosomal recessive bestrophinopathy (ARB). *Doc Ophthalmol* 2009;118(3):239-246.
23. MacDonald IM, Gudiseva HV, Villanueva A, Greve M, Caruso R, Ayyagari R. Phenotype and genotype of patients with autosomal recessive bestrophinopathy. *Ophthalmic Genet* 2012;33(3):123-129.
24. Preising MN, Pasquay C, Friedburg C, et al. [Autosomal recessive bestrophinopathy (ARB): a clinical and molecular description of two patients at childhood]. *Klin Monbl Augenheilkd* 2012;229(10):1009-1017.
25. Boon CJ, van den Born LI, Visser L, et al. Autosomal recessive bestrophinopathy: differential diagnosis and treatment options. *Ophthalmology* 2013;120(4):809-820.
26. Wang M, Sander B, la Cour M, Larsen M. Clinical characteristics of subretinal deposits in central serous chorioretinopathy. *Acta Ophthalmol Scand* 2005;83(6):691-696.
27. Bitner H, Schatz P, Mizrahi-Meissonnier L, Sharon D, Rosenberg T. Frequency, genotype, and clinical spectrum of best vitelliform macular dystrophy: data from a national center in Denmark. *Am J Ophthalmol* 2012;154(2):403-412.
28. Soliman W, Sander B, Hasler PW, Larsen M. Correlation between intraretinal changes in diabetic macular oedema seen in fluorescein angiography and optical coherence tomography. *Acta Ophthalmol* 2008;86(1):34-39.
29. Saidha S, Sotirchos ES, Ibrahim MA, et al. Microcystic macular oedema, thickness of the inner nuclear layer of the retina, and disease characteristics in multiple sclerosis: a retrospective study. *Lancet Neurol* 2012;11(11):963-972.
30. Zhu M, Zheng L, Ueki Y, Ash JD, Le YZ. Unexpected transcriptional activity of the human VMD2 promoter in retinal development. *Adv Exp Med Biol* 2010;664(1):211-216.
31. Rufiange M, Dassa J, Dembinska O, et al. The photopic ERG luminance-response function (photopic hill): method of analysis and clinical application. *Vision Res* 2003;43(12):1405-1412.
32. Hennessy MP, Vaegan. Amplitude scaling relationships of Burian-Allen, gold foil and Dawson, Trick and Litzkow electrodes. *Doc Ophthalmol* 1995;89(3):235-248.
33. Schatz P, Preising M, Lorenz B, Sander B, Larsen M, Rosenberg T. Fundus albipunctatus associated with compound heterozygous mutations in RPE65. *Ophthalmology* 2011;118(5):888-894.
34. Schatz P, Klar J, Andreasson S, Ponjavic V, Dahl N. Variant phenotype of Best vitelliform macular dystrophy associated with compound heterozygous mutations in VMD2. *Ophthalmic Genet* 2006;27(2):51-56.
35. Borman AD, Davidson AE, O'Sullivan J, et al. Childhood-onset autosomal recessive bestrophinopathy. *Arch Ophthalmol* 2011;129(8):1088-1093.

FIGURE CAPTIONS

Figure 1. Danish family with biallelic mutations in *BEST1*. Top panel. Pedigree. M refers to mutated allele whereas + refers to wild type allele. For each individual, the two *BEST1* copies are boxed. Each copy contains data of three sequence changes. Please note that only the index case (marked with an arrow) has two *BEST1* gene copies that carry missense changes (e.g. compound heterozygous), while his brother inherited two normal gene copies and the three other family members carry one normal copy of the gene and one copy with a missense change (e.g. heterozygous). Bottom panel: Chromatogram of a novel 15 base pair deletion (c.713del15) in the *BEST1* gene. The deletion (boxed) includes the two last nucleotides of exon 6 (upper part of panel) and the first 13 nucleotides of intron 6. Please note that due to sequence identity of 7 base pairs between the mutated and the wild-type sequence at the deletion border, the splice-site is not predicted to be affected by the deletion. The sequence of the index case who is heterozygous for this mutation is depicted (lower part of panel) as a chromatogram. Each nucleotide is presented with a unique color. The upper chromatogram represents an individual with two wild-type copies and therefore a single nucleotide is obtained at each position. The lower chromatogram of the heterozygous individual is a mixture of two alleles, one is wild-type and the second one contains the 15 base-pair deletion. Wt= wild type.

Figure 2. Fundus imaging of the 10 year-old index case with autosomal recessive bestrophinopathy. Top panel. Fundus image of right and left eyes of, demonstrating widespread vitelliform alterations in the posterior pole and central pigment irregularities. Middle panel. Autofluorescence imaging of right and left eyes demonstrating hyperautofluorescence corresponding to vitelliform fundus changes and hypoautofluorescence corresponding to pigment irregularities in both fundi. Bottom panel. Transfoveal optical coherence tomography scans in right and left eyes demonstrating subtle cystoid macular edema in the inner nuclear layer, subretinal mounds on Bruch´s membrane and retinal pigment epithelium and subretinal fluid with precipitate like alterations on the outer retinal surface and photoreceptor outer segments. Red arrows indicate the boundaries of the inner nuclear layer.

Figure 3. Multifocal electroretinography in a family with biallelic *BEST1* mutations. Top Left panel. The mother of the index case who is heterozygous for p.Q238L has focally reduced central responses but also a somewhat noisy recording due to artefact. Top Center. The father of the index case has regular responses throughout the posterior pole. Top Right. The sister of the index case has regular responses throughout the posterior pole. Bottom panel: right and left eyes of index case. Multifocal electroretinography amplitudes are reduced in the center but more preserved in the paracentral area in the index case. Recordings from the left eye of the index case are somewhat distorted by noise and blink artefacts and are more reduced than in the right eye.

Figure 4. Electro-oculography in right and left eyes in family with biallelic mutations in *BEST1*. Left Outer panel: Mother (heterozygous for p.Q238L). Left Inner panel. Father

(heterozygous for the p.A195V mutation). Right Inner panel. Sister (heterozygous for p.Q238L). Right Outer panel. Index case (biallelic mutations in *BEST1*). Whereas the light rise is present but reduced in the mother and sister, there is no consistent rise in light in the electro-oculography of the index case (enhanced by red dotted lines, which are flat, for the continuous recording for the right eye). The calculated light peak/dark through ratio in the index case seems falsely elevated (Table 1) which may be caused by imperfect saccades. The father presents with a normal electro-oculography light rise and light peak (enhanced by the slope of the red dotted lines for the continuous recording and by red arrows corresponding the rise of the standing potential for the right eye).

Figure 5. Full-field electroretinography (corresponding to Table 2) in family with biallelic mutations in *BEST1*. Left Outer panel: Mother (heterozygous for p.Q238L). Left Inner panel. Father (heterozygous for the p.A195V mutation). Center panel. Sister (heterozygous for p.Q238L). Right Inner panel. Right eye of index case (biallelic mutations in *BEST1*). Right outer panel. Left eye of index case (biallelic mutations in *BEST1*). A somewhat reduced rod driven response was demonstrated in the index case compared to other family members. Cone driven responses were better preserved except for a delay in 30 Hz flicker implicit time in the full-field electroretinogram. ms=milliseconds. µV=microvolts. OD=right eye. OS=left eye.

Figure 6. Full-field electroretinography luminance-response series in family with biallelic mutations in *BEST1*. Left Outer panel. Mother (heterozygous for p.Q238L). Left Inner panel. Father (heterozygous for the p.A195V mutation). Center panel. Sister (heterozygous for p.Q238L). Right Inner panel. Right eye of index case (biallelic mutations in *BEST1*). Right Outer panel. Left eye of index case (biallelic mutations in *BEST1*).ms=milliseconds. µV=microvolts. OD=right eye. OS=left eye. With increasing stimulus luminance the amplitude of the a and b waves increase, but after a further increase in luminance, there is a subsequent decrease in the b wave amplitude (photopic hill phenomenon). Full-field electroretinography responses from the left eye of the index case are somewhat distorted by blink artefact. A further analysis and comparison of amplitudes is presented in Fig. 7.

Figure 7. A graphic representation of full-field electroretinography luminance-response series in members of the family with biallelic mutations in *BEST1*. The compound heterozygous index case demonstrates a progression in the luminance-response series which at least at higher luminances does not seem to differ much from that of single heterozygous family members, indicating preserved cone function. The left eye of the index case actually demonstrates a steady increase in response with increasing luminance. Interocular asymmetry in response may be caused by muscle activity or difference in position of the Dawson-Trick-Litzkow electrotes that were used for the recording of the full-field electroretinogram.

Figure 8. Anti-Bestrophin 1 immunohistochemistry in human eyes shows strong retinal pigment epithelium-specific staining. Two adult human eyes, enucleated because of a malignant tumor (top panel) and ocular trauma (middle panel) were stained using mouse anti-Bestrophin 1 antibody. Top panel. Specimen from eye enucleated due to malignant tumor. Middle panel. Specimen from eye enucleated due to trauma. In both cases, intense fluorescent signal was restricted in retinal pigment epithelium layer. No evidence for expression of Bestrophin in other retinal layers was observed. Lower panel – negative control (human retinal section stained without primary antibody) showed no Bestrophin 1 expression. Nuclei are counterstained with 4,6-diamidino-2-phenylindole (blue). Original magnification x40.

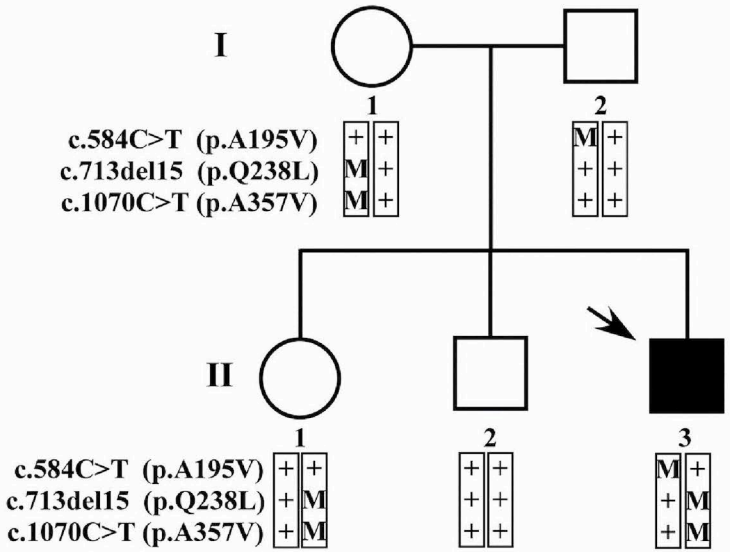
I
1
2
c.584C>T (p.A195V)
c.713del15 (p.Q238L)
c.1070C>T (p.A357V)
II
1
2
3

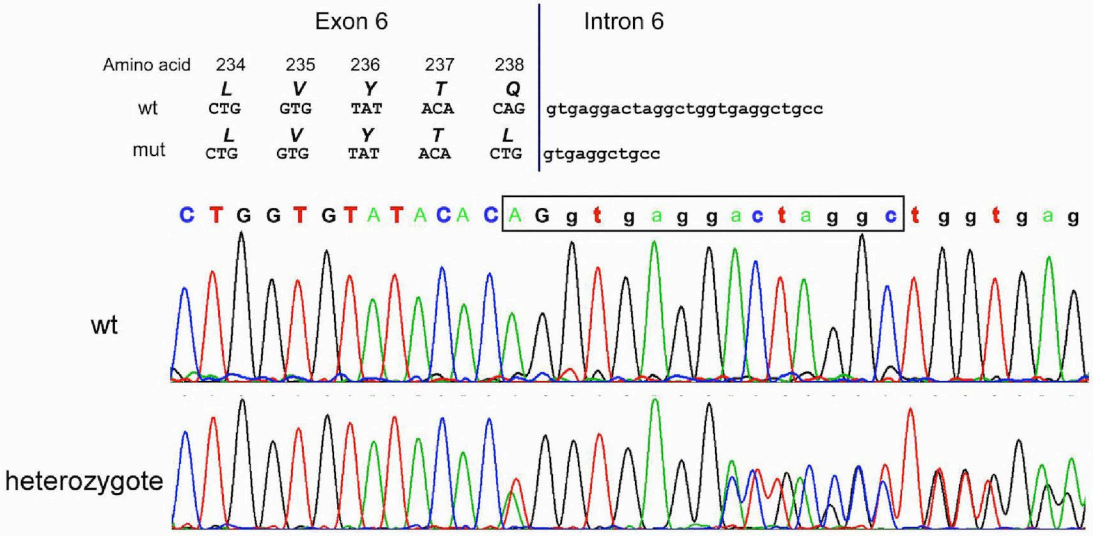
Exon 6
Intron 6
Amino acid 234 235 236 237 238
wt L V Y T Q
CTG GTG TAT ACA CAG gtgaggactaggctggtgaggctgcc
mut L V Y T L
CTG GTG TAT ACA CTG gtgaggctgcc
wt
heterozygote

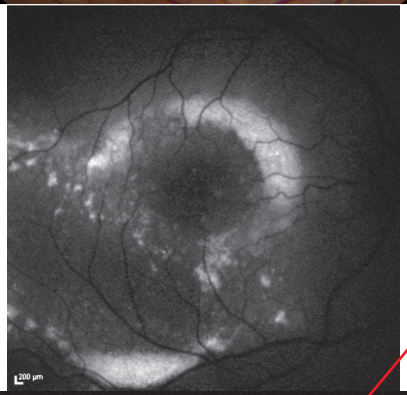
200 µm


200 µm

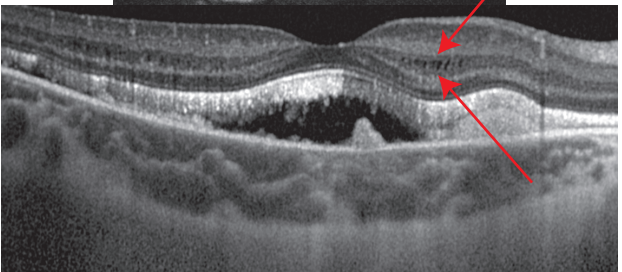

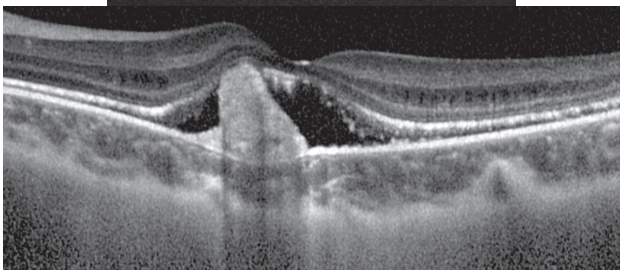

Mother of index case

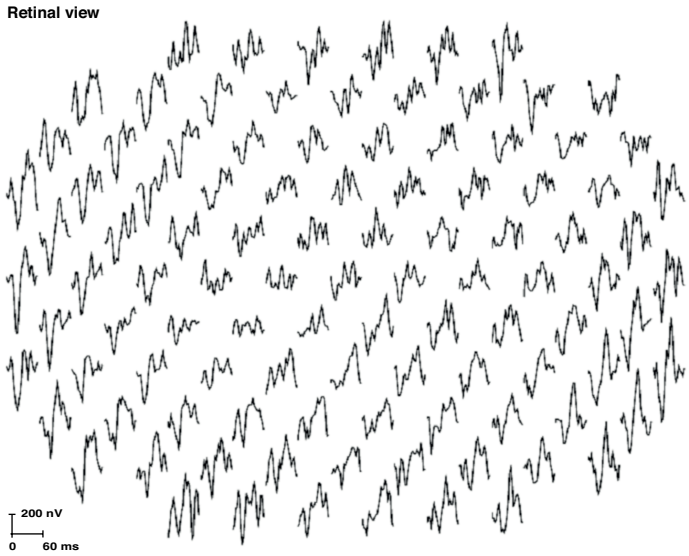

Father of index case

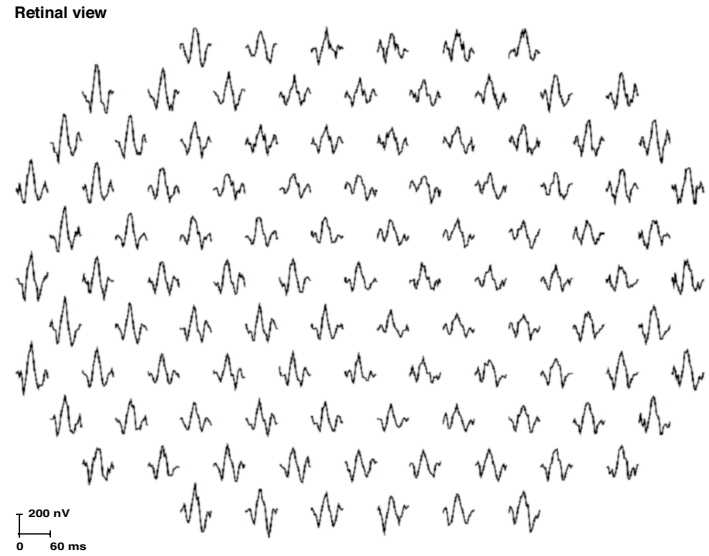

Sister of index case

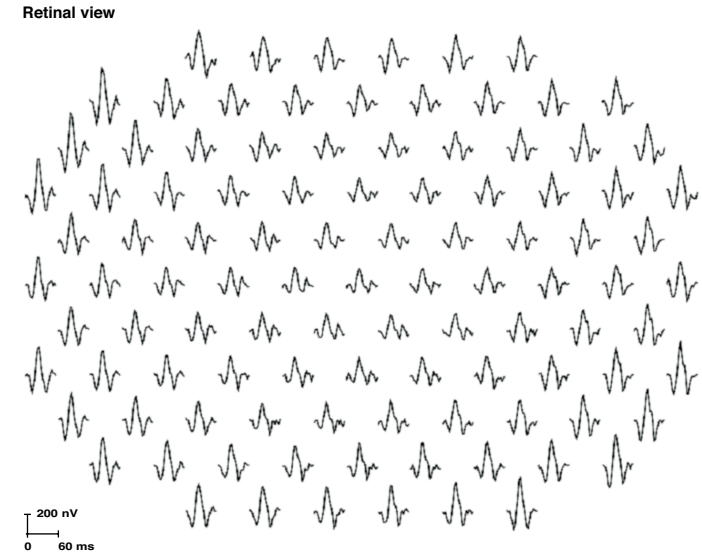

Index case, right eye (OD)

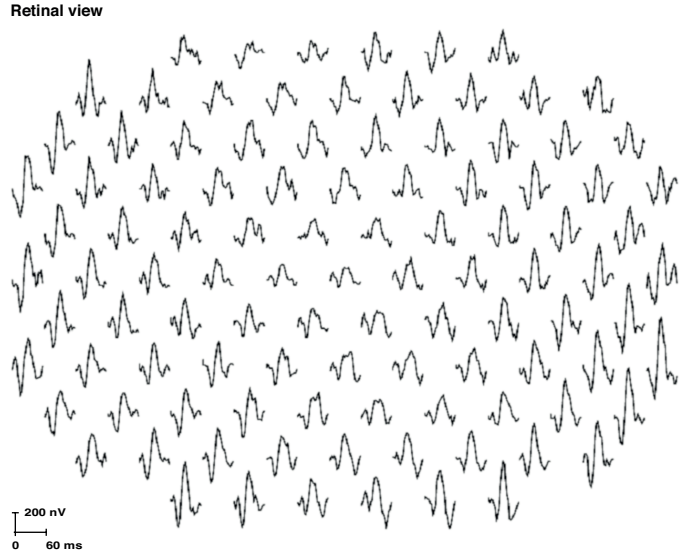

Index case, left eye (OS)

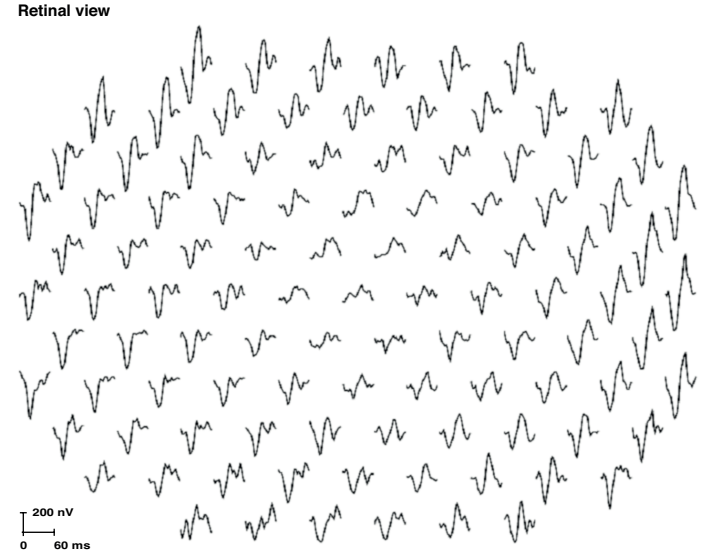

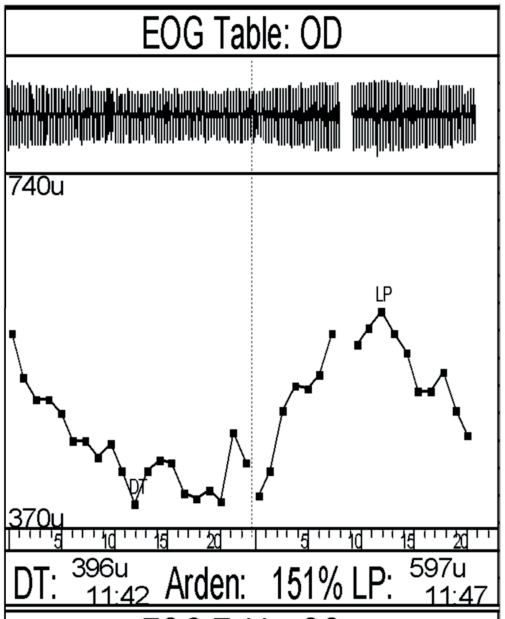

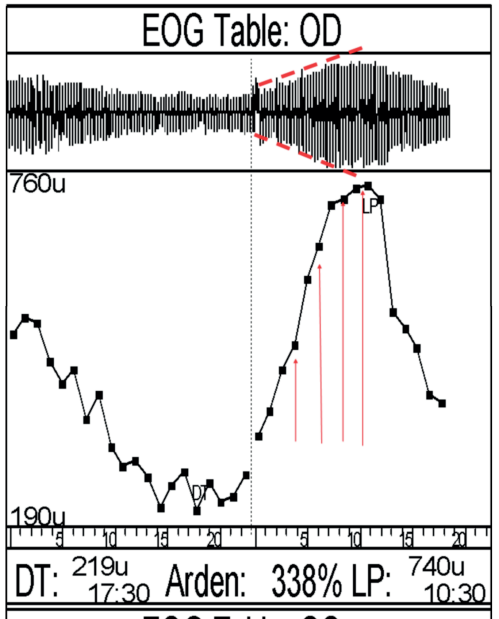

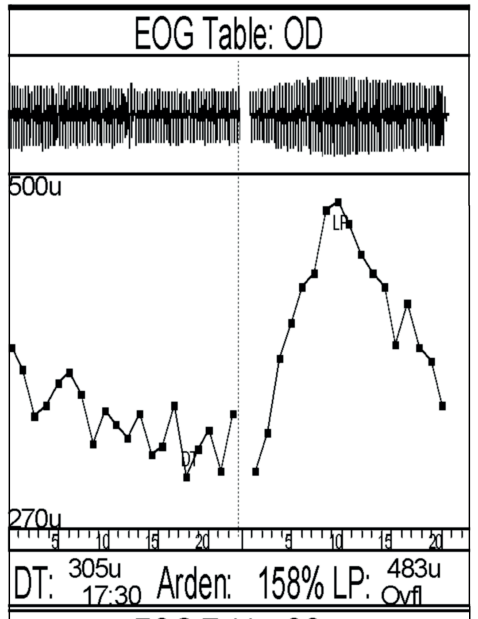

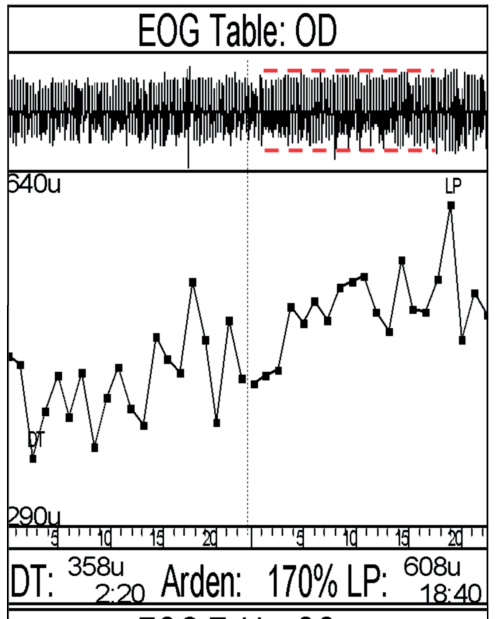

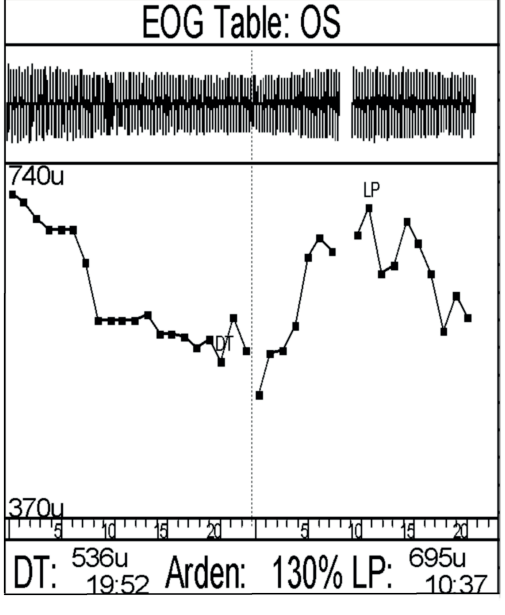

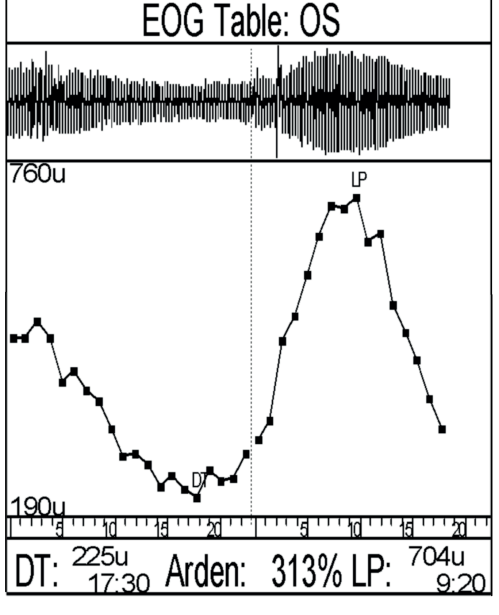

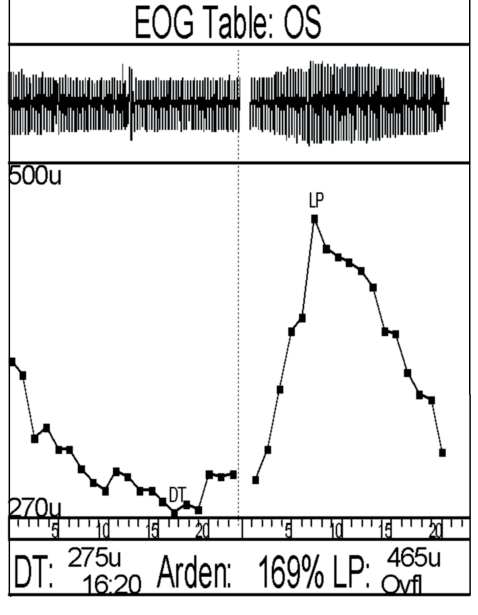

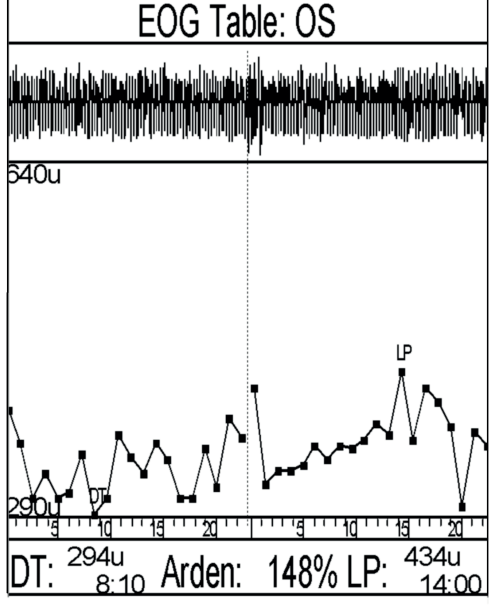

Mother of index case

Father of index case

Sister of index case

Index case

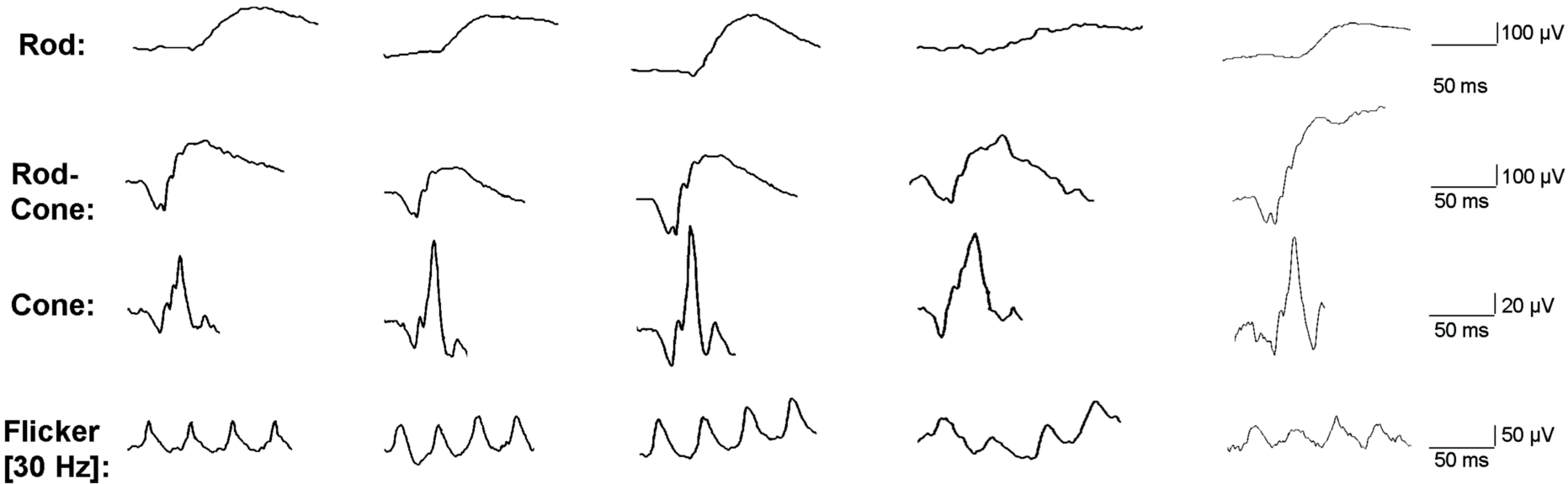
Rod:
Rod-
Cone:
Cone:
Flicker
[30 Hz]:
100 µV
50 ms
100 µV
50 ms
20 µV
50 ms
50 µV
50 ms
Mother of
index case
Father of
index case
Sister of
index case
Index case
OD
Index case
OS

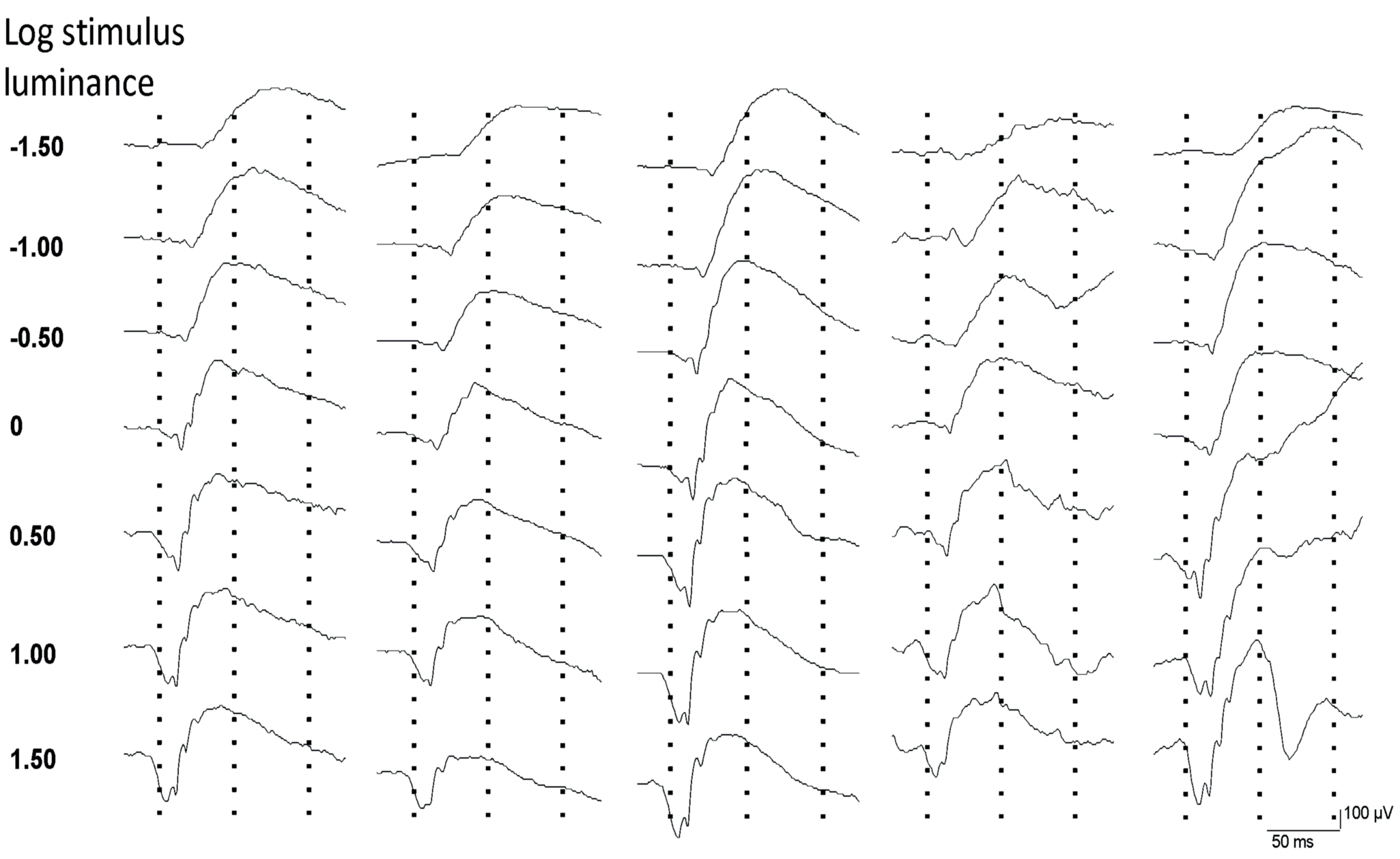
Log stimulus luminance
-1.50
-1.00
-0.50
0
0.50
1.00
1.50
100 µV
50 ms
Mother of index case
Father of index case
Sister of index case
Index case OD
Index case OS

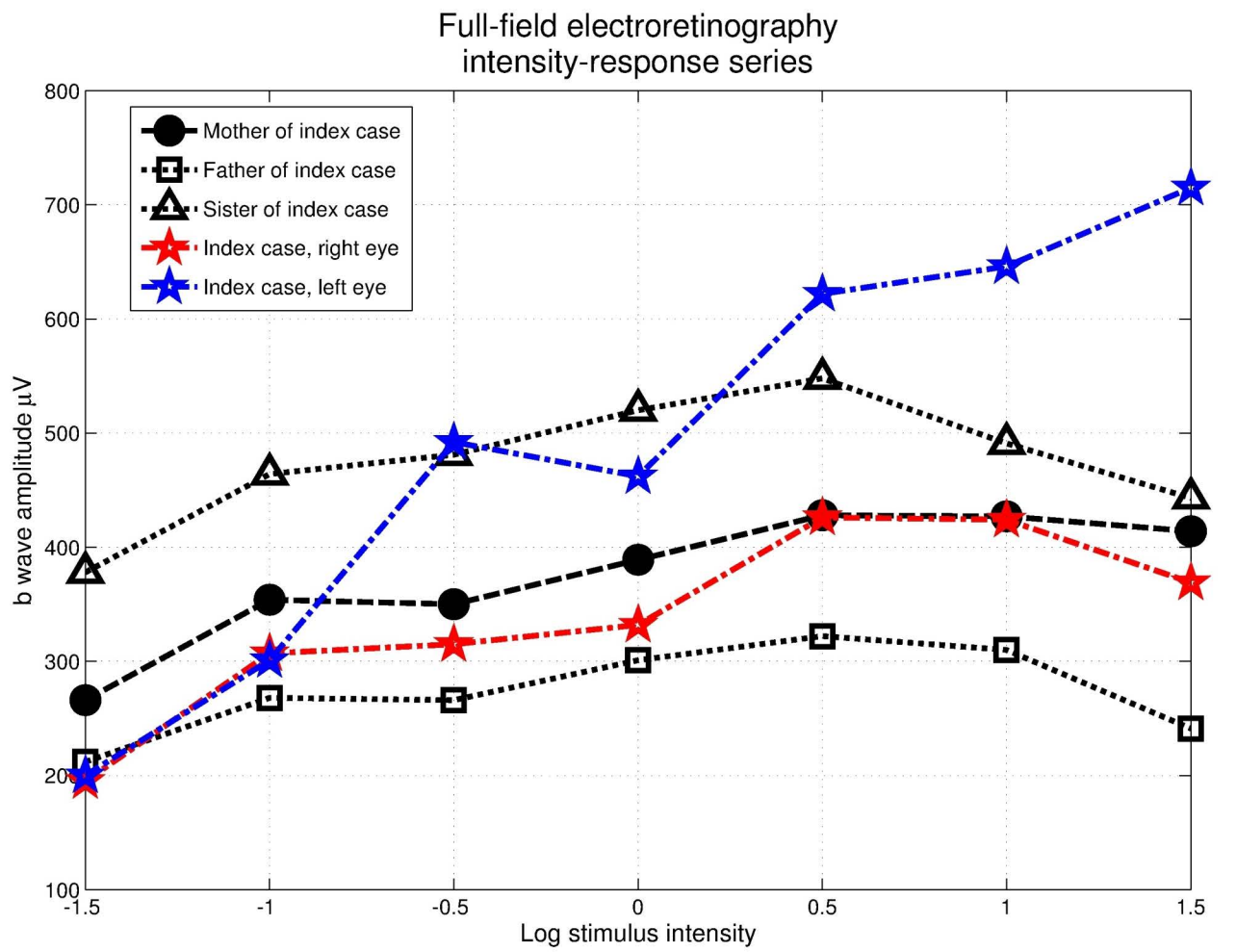
Full-field electroretinography
intensity-response series
Mother of index case
Father of index case
Sister of index case
Index case, right eye
Index case, left eye
b wave amplitude µV
Log stimulus intensity
800
700
600
500
400
300
200
100
-1.5
-1
-0.5
0
0.5
1
1.5

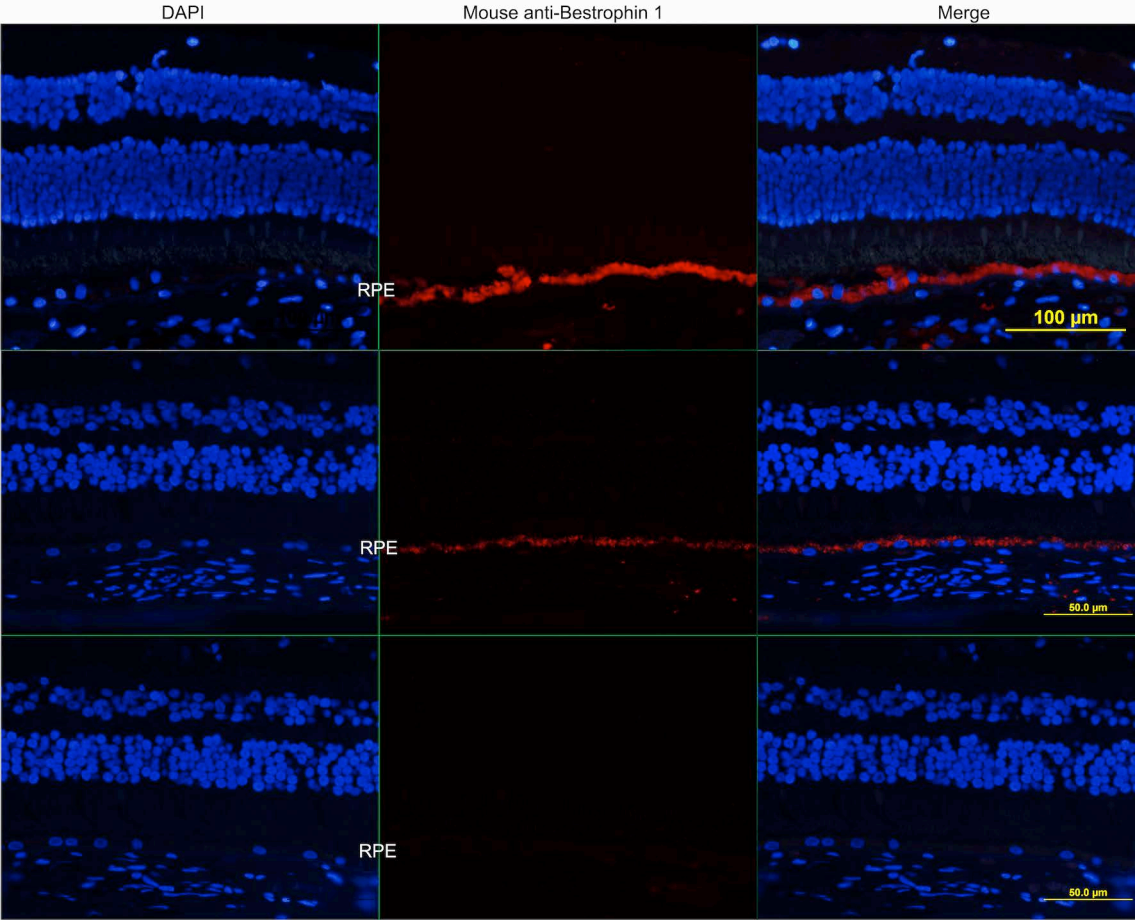
DAPI
Mouse anti-Bestrophin 1
Merge
RPE
RPE
RPE
100 µm
50.0 µm
50.0 µm

Table 1. Genetic and clinical data of each participant of family with biallellic mutations in *BEST1*.

Patient	Gender (age)	BEST1 genotype	Multifocal electroretinography amplitude ring averages for P1 wave Ring 1-2, 3-6, ring ratio[b] (nV/deg^2)	Electrooculogram Arden ratio (OD, OS)	Visual acuity OD, OS (refraction)	Subfoveal Choroidal thickness OD, OS (μm)	Anterior chamber depth OD,OS (mm)	Anterior chamber angle OD temporal, nasal (degrees)
I:1	F (51)	+ / Q238L and A357V	59.4, 28.1, 2.1 (OD)	1.51, 1.30	1.3, 1.3 (-1)	512, 464	2.33, 2.34	26.1, 20.0
I:2	M (51)	+ / A195V	62.1, 26.6, 2.3 (OD)	3.38, 3.13	1.3, 1.3 (0)	249, 288	3.65, 3.60	41.7, 39.2
II:1	F (27)	+ / Q238L and A357V	56.0, 32.4, 1.7 (OD)	1.58, 1.69	1.3, 1.3 (0)	Not analyzed	3.65, 3.72	31.5, 28.2
II:2	M (23)	+ / +	Not analyzed	Not analyzed	1.3, 1.8 (-2.5)	Not analyzed	Not analyzed	Not analyzed
II:3	M (10)	A195V / Q238L and A357V	49.9, 37.5, 1.3 (OD) 23.8, 12.3, 1.9 (OS)	1.70, 1.48	0.9, 0.28 (+1)	281, 219	3.48, 3.52	41.1, 44.6
Normal median (range)[a]			71.3 (63.6–95.0), 38.3 (20.6–46.3), 2.14 (1.60, 3.36)			342 (73-691)[17]		

[a] Normal data were obtained with a Dawson-Trick-Litzkow electrode at the Kennedy Center, based on the investigation of 10 eyes of 8 controls, age range 30-60 years.

[b] Multifocal electroretinography ring ratio is given as ring 1-2 amplitude average divided by ring 3-6 amplitude average.

Abbreviations: OD=right eye. OS=left eye. μm=micrometers. mm= millimetres. nV/deg^2= Nanovolts per degree squared.

Table 2. Full-field electroretinographic analysis of retinal function in a family with biallelic mutations in *BEST1*

Patient (family)	Gender (age)	BEST1 mutation	Full-field electroretinography									
			Rod b wave		Rod-cone a wave		Rod-cone b wave		Cone b wave		30 Hz flicker	
			Amplitude	Implicit time	Amplitude	Implicit time	Amplitude	Implicit time	Amplitude	Implicit time	Amplitude	Implicit time
I:1 (OD)	F (51)	+ / Q238L and A357V	266	86	176	22	427	55	92	32	94	28
I:2 (OD)	M (51)	+ / A195V	212	81	160	22	310	56	131	33	125	29
II:1 (OD)	F (27)	+ / Q238L and A357V	378	86	220	22	491	56	170	30	124	27
II:2 (N/A)	M (23)	+ / +	N/A									
II:3 (OD)	M (10)	A195V / Q238L and A357V	195	101	160	23	424	57	124	33	80.8	30
II:3 (OS)	M (10)	A195V / Q238L and A357V	200	79.0	158	23	646	62	143	32	98	31.5
Normal median, (range)[a]			263 (193-405)	81.5 (64.5-93)	229 (187-269)	20.5 (15.5-23.0)	479 (322-501)	42.5 (35.0-59.0)	157 (105-168)	42.3 (24.5-62.5)	135 (83.7- 165)	27.0 (24.5-29.0)

The data presented in the table correspond to Fig. 5. Rod responses were obtained after dark adaptation for 30 minutes. Cone responses and 30-Hz flicker responses were obtained after 10 minutes of light adaptation.

[a] Normal material obtained with Dawson-Trick-Litzkow electrode, at the Kennedy Center, based on the investigation of 9 eyes of 8 controls, age range 30-60 years.

Abbreviations: OD=right eye. OS=left eye. Amplitude is given in μV=microvolts. Implicit time is given in milliseconds. N/A= not analyzed.

Supplementary Table 1: Details about the *BEST1* sequence changes identified in this study in a family with biallelic mutations in *BEST1*.

Mutation name (cDNA level)	Exon number	Mutation name (protein level)	MAF (based on 1000 Genomes)[a]	PolyPhen2 prediction[b]	MutationTaster prediction[c]	Reference	rs number in dbSNP[d]
c.584C>T	5	p.Ala195Val	0.001	0.992 probably damaging	0.998 disease causing	[19-23]	rs200277476
c.713del15	6	p.Gln238Leu	0	1.000 Probably damaging	1.000 disease causing		
c.1070C>T	9	p.Ala357Val	0.003	0.049 benign	0.999 polymorphism		rs17854138

[a] None of the variants appears in the evs (Exome Variant Server) database (http://evs.gs.washington.edu/EVS/ accessed: September 3, 2013) including data of about 13,000 chromosomes. MAF- Minor allele frequency.

[b] http://genetics.bwh.harvard.edu/pph2/ accessed: November 26, 2013.

[c] http://www.mutationtaster.org/ accessed: November 26, 2013.

[d] dbSNP-Single Nucleotide Polymorphism Database: http://www.ncbi.nlm.nih.gov/SNP/ accessed: November 26, 2013.